Received 14 May 2023, accepted 31 May 2023, date of publication 6 June 2023, date of current version 21 June 2023.
Digital Object Identifier 10.1109/ACCESS.2023.3283369

RESEARCH ARTICLE

Performance Analysis of 5G-R Network Bearing Train Control Information of HSR Based on Hardware-in-the-Loop Simulation

YIQUN LIANG [1,2,3], HUI LI [2,3], YI LI [2,3], ANNING LI [2,3], YUNQI WANG [1], AND DE LI [4]
[1]Postgraduate Department, China Academy of Railway Sciences, Beijing 100081, China
[2]Signal and Communication Research Institute, China Academy of Railway Sciences Corporation Ltd., Beijing 100081, China
[3]National Research Center of Railway Intelligence Transportation System Engineering Technology, Beijing 100081, China
[4]Beijing Huatie Information Technology Company Ltd., Beijing 100081, China
Corresponding author: Hui Li (tkthlh@sina.com)

This work was supported in part by the Science and Technology Research and Development Program of China State Railway Group Company Ltd., under Grant P2021G053 and Grant SY2021G001; and in part by the Science and Technology Research and Development Program of China Academy of Railway Sciences Company Ltd., under Grant 2021YJ085 and Grant 2022YJ033.

ABSTRACT Train Control system as the nerve of railway has attracted significant attention from both academia and industries since it is closely related to safety, especially in High-speed railway(HSR). To be in line with the research of 5G network for railway (5G-R), which is a topic of common concern for railways around the world, performance of 5G-R bearing train control information needs to be studied to ensure high-quality of transmission. In this article, the train-ground communication demand for train control is deeply analyzed, and three scientific questions are extracted, involving the service establishment latency of the train control on-board modules, the end-to-end data transmission latency distribution, as well as the redundant communication link switching algorithm under network abnormal conditions. A hardware-in-the-loop simulation environment combining the actual 5G-R system and channel simulator is built, under which, 95% statistical value of service establishment is analyzed, which is furtherly used to determine length of transition section between 5G-R and GSM-R. End to end latency samples are collected and the statistical distribution is analyzed with χ^2 fitting test method, and statistically modeled by Student t-distribution. Moreover, in order to maintain a reliable communication link, based on the heartbeat information of dual train-ground links, a better link decision algorithm using Informer Long Sequence Time-Series Forecasting(LSTF) method is proposed, and verified with normal as well as abnormal latency samples by caculating MAPE values. Relevant research results of this article will be helpful for facilitating the design of future train control and 5G-R system.

INDEX TERMS 5G-R, channel model, CTCS, ETCS, fitting test, HSR, informer, LSTF, train control.

I. INTRODUCTION

European Train Control System(ETCS) is the signalling element of the European Rail Traffic Management System which includes the control of train movement authorities, automatic train protection and the interface to interlockings [1]. China Railway has also proposed the Chinese Train Control System(CTCS). Currently, ETCS and CTCS systems have been deployed all over the world, especially for high-speed lines. Train control system plays an important role in improving the level of railway transportation automation, improving efficiency and ensuring the safety of transportation.

Both ETCS and CTCS have different levels. As the highest level currently in use, ETCS-2 and CTCS-3 system use GSM-R as train-ground information transmission bearer network. As a broad consensus, GSM-R, of which the first implementation was launched in 1999, has been a great success, more than 100,000 km of railway tracks are daily operated through GSM-R. However, GSM-R is a narrowband

The associate editor coordinating the review of this manuscript and approving it for publication was Parul Garg.

system, the approximately cell rate is about 100 kbps, which is unable to meet the constantly evolving demand for vehicle-ground transmission bandwidth. What's more, from the perspective of industrial chain, GSM-R products and related technical support are also facing the problem of life cycle, with an end of support for GSM-R planned by 2030 [2].

These considerations led UIC, as soon as 2012, to launch the first studies for a successor to GSM-R, pertinently named Future Rail Mobile Communications System (FRMCS) [2]. In 2011, China Railway started the research of the next generation radio-communication system. And in 2015, the Next Generation Radio-communication Working Group of CHINA RAILWAY(NGCR), was established, including 5 sub-working groups, which focus on spectrum, standard, service, industry, test respectively.

In the meanwhile, on June 6, 2022, 3GPP Release 17(R17)) standard, namely the third full version of the 5G NR standard, has been officially frozen, marking that the enhanced functions of the 5G system have been implemented with complete technical support, and 5G technology and standards have entered a mature and stable period. The global 5G network has developed steadily. By the end of the third quarter of 2022, 224 operators in 91 countries and regions around the world have launched commercial 5G networks based on the 3GPP standard. In the third quarter of 2022, 6 new 5G commercial networks have been added globally. It is estimated that by the end of 2022, the number of global 5G commercial networks will exceed 230 [3]. Considering the maturity of 5G standard and industrial chain, both UIC and China Railway have adopted 5G standard for the future railway mobile communication system, Japan and the Republic of Korea have also conducted railway related 5G tests.

In its latest version of FRMCS user requirements specification, UIC described the importance of a reliable communication bearer in order to ensure efficient data transmission between the on-board and the ground system(e.g., ETCS,CTCS) [4]. In the future, train control application will be a key application for 5G-R, and 5G-R network will provide train control system with lower latency, larger capacity and higher reliability.

Scholars have carried out a series of related research work. In the era of GSM-R, the control and signalling information between the train and the related ground control center, is transmitted via a circuit-switched and wireless approach, which is a connection-oriented system, in which a static channel was allocated to each wireless user. A deadlock of the system may be caused if the number of users rapidly increases. In order to solve this problem, and taking into account that the GSM-R infrastructure, which has already been installed by the national railway operators, should continue to be used in a certain period, to save the high capital investment of these railway operators, GPRS was introduced and investigated [5]. In Europe, during 2012∼2016, laboratory and field tests of GPRS bearing ETCS-2 information was carried out, and corresponding standards were revised [6]. In [7], QoS key metrics of GPRS based CTCS-3 train control safety data transmission was proposed. By using the QoS measurement methodology of hard-in-the-loop simulation test bench, statistical regularities of transfer delay of UDP frame, error or lost frame as well as GPRS attachment and Packet Data Protocol(PDP) context activation were offered.

With respect to research of next generation mobile communication network, UIC conducted relevant research, which include railway needs and communication system functionalities, defining the targeted architectures and evaluating the candidate technologies, as well as spectrum issues, besides, a special group named TOBA was set to investigate the architecture of the FRMCS on-board system [8]. In 2020, Korea Railroad Research Institute(KRRI) announced the successful testing of 5G-based autonomous train control technology at its dedicated test track in Osong, using 5G communications helps to reduce the transmission delay between trains, whilst improving both the data transmission capacity and reliability up to 20-fold compared to GSM-R. It is estimated that using of train-to-train communications could reduce headways by up to 30%, to a minimum of around 60 s [9].

The high-speed railway(HSR) propagation channel has a significant impact on the design and performance analysis of wireless railway control systems [10]. When the speed of the train is over 300 km/h, the wireless channel exhibits rapidly time-varying and nonstationary features [11], [12]. In [13], impact of Doppler shift to the railway dedicated mobile communication quality was analized, and a Doppler shift measurement approach which correctly reflects the time-varying characteristic of the channel was proposed. The differences between radio communication protocols based on GSM-R network and 5G-R network were compared and analyzed from the aspects of protocol function, transmission reliability and transmission rate, the conclution that the radio communication protocol based on 5G-R network has higher reliability and faster transmission rate was drawn [14].

In [15], CTCS-3 train control system scheme based on 5G-R network was studied, interface interconnection scheme between 5G-R network and train control system was highlighted, the 5G-R network settings, engineering deployment and communication process in the complex scenarios of RBC handover boundaries were investigated in detail. Onboard radio of train control system was designed based on embedded system in [16], architecture, interface with ATP, AT Command, connection establishment and data transmission process were expounded.

Deterministic and stochastic Petri nets(DSPN) formal modeling tool was commonly used to analyze reliability of the 5G-R network. In [6], the 5G-R wireless communication fault model and the train-ground communication scenario model of the train control system were built respectively, according to the laboratory test data, parameter selection of DSPN model was completed, and non-fault probability of train-ground communication link as well as reliability index of the train-ground communication data transmission were analyzed through simulation. DSPN was also used in the reliability analysis of Communication-based train control(CBTC) systems, in [17], a laboratory test environment testing the next generation CBTC data communication system performance was set up, and the performance data was converted as DSPN model parameters to evaluate the system reliability, including both reconnection and handover scenarios. In [18], the authors focused on probabilistic analytical expressions of several conditions, such as packet error rate, long handover execution time, and connection loss that lead to a train control system service interruption, and the accuracy of this analytical approach was proved when the results were compared with those given by a simulation approach with a Petri net model. Considering the high reliability requirements of train-ground data transmission for train control, both ETCS and CTCS choose TCP/IP protocol as the data transmission layer protocol stack. In [19], the authors investigated the performance and behavior of TCP/IP in a high speed environment with a peak speed of 310 km/h, performance metrics, such as Round Trip Time(RTT), packet loss rate, and throughput were analysed, the results show that RTT and packet loss rate increase significantly and throughput drops considerably in high speed situations. In [20], authors conducted in-depth examination of the performance of two widely deployed congestion control algorithm of transport-layer protocols: TCP CUBIC and TCP BBR, and based on BBR a simple yet effective congestion control algorithm was designed to further boost the throughput by up to 36.5%. The communication delay of train control services has a great impact on the safty and design of the train control system. In [21], the instantaneous data rate of the wireless channel was characterized by a semi-Markov modulated process, which took into account the channel variations due to both large-scale and small-scale fading effects, and the stochastic upper delay bounds of train control services were derived with both the moment generating function method and the complementary cumulative distribution function method.

5G-R network adopts packet switching technology, it is significantly different from GSM-R system with respect to business flow and quality of service management. To the best of the author's knowledge, although much remarkable progress has been achieved, there is no publicly reported papers to discuss in detail performance of 5G-R network bearing train control information, under typical railway scenarios of wireless communication channel and high-speed conditions, in terms of service establishment, data transmission, as well as communication link keeping stage. To fill the aforementioned research gaps, the aim of this paper is to deeply analyzed the train-ground communication demand, base on which, 3 scientific questions, which are the registration and service establishment latency of the train control on-board modules, the end-to-end data transmission latency distribution, as well as the redundant communication link switching under network abnormal conditions, are proposed and analyzed in our fairly built hardware-in-the-loop simulation environment combining the actual 5G-R system and channel simulator.

The rest of this paper is structured as follows. In section II, we will decribe the train-ground communication demand for train control. The simulation environment and methods to solve the 3 scientific questions will be presented in Section III. Then corresponding analysis results are summarized in Section IV. Finally, Section V will present the conclutions and highlight the futher research works.

The abbreviations listed in Table. 1 are used in this manuscript:

TABLE 1. Abbreviations used in this manuscript.

Abbreviations	Full Name
3GPP	The 3rd Generation Partnership Project
5G-R	5G For Railway
5QI	5G QoS Identifier
AOA	Azimuth angle Of Arrival
AOD	Azimuth angle Of Departure
ARP	Allocation Retention Priority
ATP	Automatic Train Protection
AWGN	Additive White Gaussian Noise
CBTC	Communication-based train control
CDL	Clustered Delay Line
CPE	Customer Premise Equipment
CSD	Circuit Switched Data
CTCS-3	Chinese Train Control System Level 3
ETCS-2	European Train Control System Level 2
FRMCS	Future Railway Mobile Communications System
GBR	Guaranteed Bit Rate
GSM-R	GSM for Railway
HSR	High-speed Railway
LOS	Line Of Sight
LSTF	Long Sequence Time-Series Forecasting
MAE	Mean Absolute Error
MAPE	Mean Absolute Percentage Error
MSE	Mean Square Error
MT	Mobile Terminal
NAS	Non-Access Stratum
PDU	Protocol Data Unit
QoS	Quality of Service
RBC	Radio Block Center
RRC	Radio Resource Control
RTT	Round Trip Time
RTU	Radio Transfer Unit
TDL	Tapped Delay Line
UIC	International union of railways
ZOA	Zenith angle Of Arrival
ZOD	Zenith angle Of Departure

II. TRAIN-GROUND COMMUNICATION DEMAND ANALYSIS FOR TRAIN CONTROL

From the perspective of whole life cycle process of 5G-R providing train-ground communication bearer for train control service, the train-ground communicatin demand for train control can be can be classified into three categories. Service establishment, the end to end data transmission of train control service and also strategy which has to be considered when the wireless channel deteriorates, these are different stages of

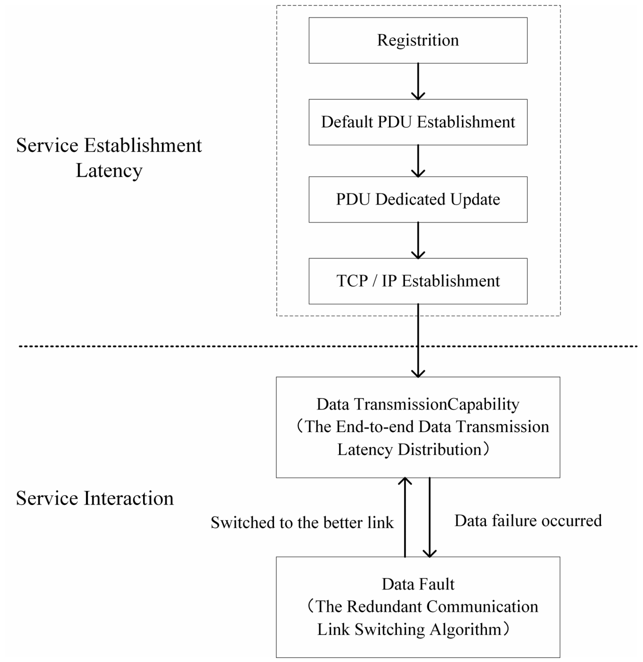

FIGURE 1. Entire lifecycle of 5G-R network bearing train control services.

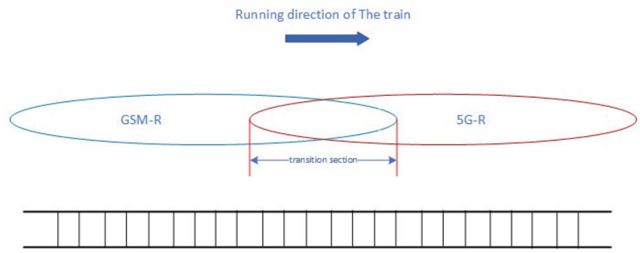

FIGURE 2. Transition section.

the entire lifecycle of the 5G-R network bearing train control services, these three scientific stages and thereby derived questions of these stages, constitute an organic integrity, and they are closely related to each other, as shown in Fig. 1. Service establishment is the premise of data transition, and the redundant communication link switching algorithm is used to maintain good channel transmission quality, thereby improving the reliability of train control services.

A. SERVICE ESTABLISHMENT LATENCY

At the initial stage of the deployment of the 5G-R network, the GSM-R network will not be completely replaced nationwide [22], instead, the 5G-R network will be deployed in the new lines, in the meanwihle, part of the existing GSM-R network covered lines of which the GSM-R equipment has reached its life cycle will be equipted with 5G-R network. Therefore, there must be a scenario of train operation in which train runs from the GSM-R network covered line to the 5G-R network covered line. For the train control on-board equipment ATP, it is best to complete the registration and service migration to the 5G-R network in the shortest time. However, the registration and service migration process of the on-board terminal to the 5G-R network needs to go through four steps, including initialization registration, default bearing PDU establishment, dedicated PDU modification [23], [24], as well as TCP/IP connection establishment. The total latency of the four steps constitutes the latency of service establishment process.

Service Establishment latency multiplied by the train operation speed is the distance required to establish services under the 5G-R network. In this distance range, which we call transition section, GSM-R and 5G-R double coverage needs to be achieved. The length of the transition section is an important parameter which needs to be considered in the network design stage. The transition section is shown in Fig. 2.

B. END TO END DATA FRAME TRANMISSION LATENCY

In order to ensure the reliable transmission of train-ground data of train control service, both the ETCS and CTCS train control systems based on packet switching adopt TCP/IP as the data link layer protocol [25], in order to carry the upper layers' services, including adaptation layer, security layer and application layer. The typical TCP/IP data frame length transmitted between train and ground is 560 bytes [26]. The train-ground data transmission latency is directly related to the effectiveness of the train control system. Mastering the TCP/IP 560 bytes train-ground transmission latency statistical rules under typical railway channel scenarios is of great significance for the design, development and reliable operation of the train control system.

C. WIRELESS COMMUNICATION LINK RELIABILITY

The train control information transmitted between the train and ground [27], such as the uplink train position report, request for shunting and the downlink movement authority, is directly related to the safety of the train operation and passengers, so the robustness of the wireless channel is particularly important.

At present, two sets of independent communication modules and antenna feeder systems are used for on-board equipment to carry out service continuity in the RBC handover area, which is the transition session mentioned above. Normally, only one module carries data transmission service. Fig. 3 describes the scenario of connection loss, in which the Rxqual and Rxlev of MT1 deteriorates until the connection is lost, and then MT2 takes over the service, and the disconnection of wireless channel finally results in an interruption of train control application layer service, which is defined as train control service time out.

The authors of [15] proposed the idea of two modules transmitting the same train control data at the same time. This solution can form link redundancy, however, it will increase the waste of air interface resources and the complexity of ground equipment's processing logic. This paper proposes a new solution, that is, two small amount heartbeat data are transmitted between train and ground equipment via two independent modules respectively at the same time, and the informer method is used to analyze the latency samples,

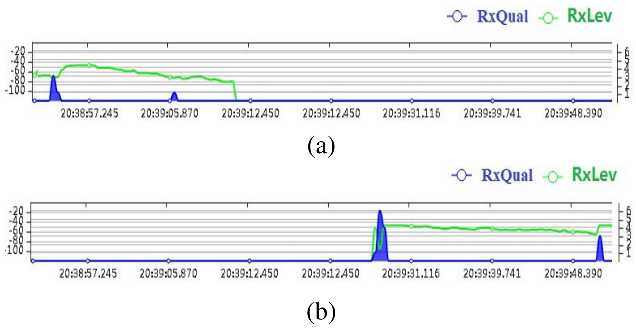

FIGURE 3. Train control service time out caused by loss of module connection. (a) Rxqual and Rxlev of MT1. (b) Rxqual and Rxlev of MT2.

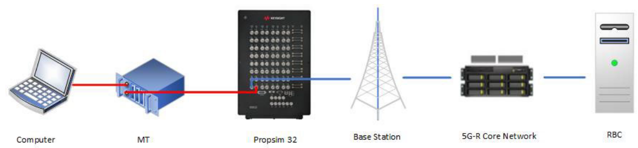

FIGURE 4. Simulation system architecture.

to further forcast the statistical law of the transmission delay of the future wireless channel, and decide the data transmission link to be used in the next step. In this way, the probability of wireless link loss will be significantly reduced.

III. SIMULATION AND ANALYSIS

A. ESTABLISHMENT OF SIMULATION ENVIRONMENT

5G-R has been adopted as the future mobile communication system by International Railway Union (UIC), and specifications such as user requirements have already been released, moreover, corresponding prototype equipments have been developed. Experimental environment is an important infrastructure for static R&D activities, low-speed train field tests for proof of concept (PoC), as well as high-speed field tests. Research institutes and companies from many countries have already built their own laboratory static 5G-R experimental environment. In the meanwhile, several countries have built low-speed train field tests environment, for instance, China has built a 9-kilometer circular railway test line with 5 5G-R base stations for 5G-R PoC test in the northeast part of Beijing, and Germany has also built a 10-kilometer railway test line in the Ore Mountains and PoC test is being conducted on this line. However, to the best of the author's knowledge, there is no high-speed 5G-R field test environment in the world, so a hardware-in-the-loop simulation system has to be built and used in our research.

The architecture of our simulation system is shown in Fig 4.

Our hardware-in-the-loop simulation system consists of mobile terminal(MT), Propsim F32 wireless channel simulator, 5G-R base station, 5G-R core network, radio block center of train control system(RBC) as well as signaling and data testing software. Among them, MT and RBC are equipment of train control system, which are connected by feeder and adjustable attenuator to the 5G-R network and channel simulator.

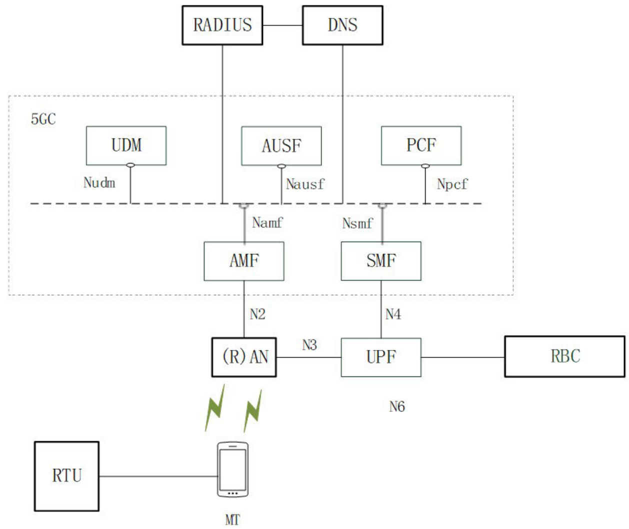

FIGURE 5. Architecture of 5G-R network.

All the Hardware equipments except the wireless channel simulator are exactly the same as the equipments which will be used in the future deployment. As for the wireless channel simulator, we choose Propsim 32 produced by Keysight company, and this channel simulator is DEKRA Certified, conforms with EN ISO/IEC 17050.1:2010, and commonly used by universities, research institutes, network operators as well as manufacturer in the channel simulation area all over the world. In order to avoid introducing of other interference signals in the channel, the simulator connects the base station and the terminal through wired feeders.

Propsim F32 wireless channel simulator has a radio frequency bandwidth of 40 MHz, supports up to 32 RF physical channel interfaces, up to 128 logical fading channels (bidirectional 8×8 MIMO), and supports a frequency range of 350 MHz-6 GHz. The maximum path delay is 3 ms, the maximum Doppler is ± 1.6 MHz, and the mobile speed is up to 500 km/h. It can achieve accurate signal fading processing in terms of time, phase, and amplitude. It contains a variety of channel models, including geometric channel modeling tools that support 3GPP Spatial Channel Model (SCM), Wireless World Initiative New Radio (WINNER) Model and user-defined models. The simulator has outstanding multi-link simulation ability. It can restore wireless channels with characteristics of different channel models, mobile speed, path loss, noise, and interference by simulating real parameters such as path loss, multipath fading, Doppler spread, delay spread, polarization, correlation, and also, it can simulate high-speed train scenarios and is suitable for railway channel simulation.

During the test, a computer connecting with the test terminal MT is used to run softward with which RRC and NAS signaling message, as well as latency samples are extracted.

1) 5G-R NETWORK CONFIGURATION

We use the real 5G-R system to build the test environment. The architecture of 5G-R network is shown in Fig. 5, which includes 5GC components, as well as access network.

TABLE 2. Typical parameters of the 5G-R network.

Parameter	Detail Information
5G NR Standard	5G FDD
Frequency	3GPP Band n1(1965-1975 MHz/2155-2165 MHz)
BandWidth	10 MHz
Subcarrier interval	15 kHz
MIMO Configuration	4T4R(BS)/1T4R(UE)
Modulation and coding mode	QPSK/16QAM/64QAM/256QAM

TABLE 3. 5G-R QoS requirements of train control.

5QI Property				
5QI	Resource Type	Priority	Packet Latency	Packet Loss Rate
65	GBR	7	75ms	1.00E-01
ARP Property				
ARP	Occcupy	Be Occupied	Be Released	-
2	Y	N	N	-

The typical parameters of the 5G-R network are listed in Table 2.

Considering the high priority requirements of train control service, it is necessary to provide high priority radio channel for train control train-ground data transmission. The parameters of 5G-R network QoS used in our configuration is listed in Table 3.

2) CHANNEL MODEL SELECTION

The simulation uses the 3GPP TR 38.901 channel model [28]. 3GPP TR 38.901 channel model is developed by 3GPP for 5G in 0.5-100 GHz frequency range. It presents four typical scenarios, namely, indoor hotspot (InH), urban macro (Uma), urban micro (Umi) and rural macro (RMa) under different frequency bands, different bandwidths and different spatial dimensions.

Since railway propagation scenario has the characteristics of fast-moving speed, small distance between base stations, complex and changeable environment (viaduct, cutting, tunnel, etc.) [29], the coverage area being distributed in a strip along the railway, and high cell handover frequency, as shown in Fig. 6, the RMa model meets the requirements of the railway scene, so it is used as the large-scale channel model of our simulation.

There may be a line-of-sight (LOS) path in the communication path between MT and base station, whereas other communication paths are defined as non-line-of-sight (NLOS) paths due to diffraction and reflection loss through buildings. The definition of LOS probability in RMa model is:

$$P_{LOS} = \begin{cases} 1 & d_{2D} \leq 10 \text{ m} \\ \exp\left(-\dfrac{d_{2D}-10}{1000}\right) & d_{2D} > 10 \text{ m} \end{cases} \quad (1)$$

The 2D and 3D distance are shown in Fig. 7:

Considering that the terrain along the high-speed railway is mainly composed of plains and viaducts, also taking into account that the coverage radius of 5G base station is about 1500 m, when d_{2D} is greater than 703.147 m, the probability of the existence of LOS is more than 50%, so there is a strong direct component in the received signal, and the LOS model is selected as the simulation channel.

FIGURE 6. Typical HSR propagation scenario.

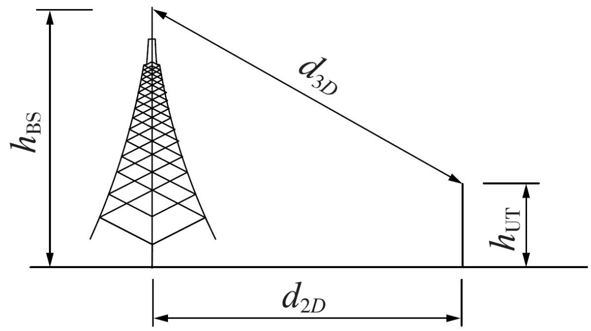

FIGURE 7. 2D and 3D distances.

$$\begin{aligned} PL_{RMa-LOS} &= 20\log_{10}(40\pi d_{3D} f_c/3) \\ &\quad + \min\left(0.03h^{1.72}, 10\right)\log_{10}(d_{3D}) \\ &\quad - \min\left(0.044h^{1.72}, 14.77\right) \\ &\quad + 0.002\log_{10}(h)d_{3D} \end{aligned} \quad (2)$$

The large-scale channel model generated by the high-speed channel simulator is shown in Fig. 8. The scene simulated in the Figure is that the train switches from one base station to another base station at a constant speed of 350 km/h, and the blue line represents the power output by the simulator at different times. When the train moves away from the base station in the left side of the Figure, the pathloss increases and the power decreases. After the train passes the cell edge, and runs to the base station in the right side of the Figure, the pathloss decreases and the power increases. The abscissa is time, the unit of which is s, and the ordinate is power, the unit of which is dBm, and a grid in the vertical direction represents 10 dBm.

In [30], the RSRP data of 5G public network along the railway are collected using a 120km/h train, and compared

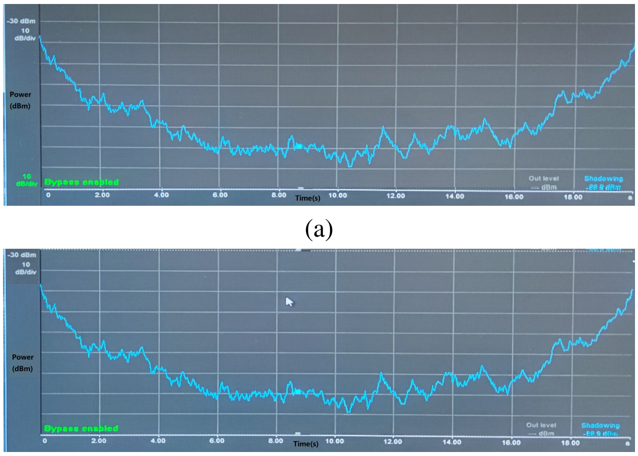

(a)

(b)

FIGURE 8. **Downlink and uplink large-scacle channel models. (a) Downlink large-scale channel model. (b) Uplink large-scale channel model.**

with the data obtained by 3GPP TR 38.901 model simulation by calculating MAPE. The result shows that the MAPE of the field test data and the data obtained by 3GPP TR 38.901 model simulation is 4.48 (< 5), which demonstrates that the two data set are consistent with each other, and can indirectly prove the reliability and accuracy of our simulation results.

In terms of small-scale channel model, CDL (Clustered Delay Line) channel model and TDL (Tapped Delay Line) channel model are defined in 3GPP standard. The TDL model mainly studies the multipath delay parameters and the Doppler parameters reflecting the time-varying characteristics of the channel. Based on the TDL model, the CDL model introduces the concept of cluster, and adds the azimuth angle of departure (AOD), azimuth angle of arrival (AOA), zenith angle of departure (ZOD), and zenith angle of arrival (ZOA) to characterize the spatial characteristics of the channel model.

According to the fact that there are fewer reflections and refractions in the railway propagation scenario compared to public network, so this paper uses a simplified TDL model. TR38.901 has five TDL models. TDL-A, TDL-B and TDL-C are three different NLOS models. TDL-D and TDL-E construct the LOS models. The model corresponding to the Rma scenario is TDL-E.

In the ITU-R report [31], three TDL models, namely TDL-i, TDL-ii and TDL-iii, are constructed to represent three different channel profiles for NLOS, while TDL-iv and TDL-v are constructed for LOS. These five models are the same as TDL-A, TDL-B, TDL-C, TDL-D and TDL-E defined in 3GPP 38. 901.

From Table. 4 [31], we can tell, ITU-R recommends the TDL-E model in the rural area and mobile scenario, which is exactly consistent with RMA scenario defined in TR 38.901.

The number of TDL-E model taps N is 14, and the normalized delay $\tau_{n,model}$ and power of each tap P_n are shown in Table 5.

TABLE 4. **Additional channel model parameters for link-level simulation.**

Scenarios	Link-level Channel model
Indoor Hotspot-eMBB(for Mobility)	NLOS:CDL/TDL-i;LOS:CDL /TDL-iv
Dense Urban-eMBB (for Mobility)	NLOS:CDL/TDL-iii;LOS: CDL/TDL-v
Rural-eMBB (for Mobility)	NLOS:CDL/TDL-ii;LOS:CDL/TDL-v
Urban Macro-mMTC(for Connection density)	NLOS:TDL-ii;LOS:TDL-v
Urban Macro- URLLC (for Reliability)	NLOS:TDL-i;LOS:TDL-v

TABLE 5. **TDL-E Model*.**

Tap #	Normalized delay in [ns]	Power in [dB]	Fading distribution
1	0 0	-0.03 -22.03	LOS path Rayleigh
2	0.5133	-15.8	Rayleigh
3	0.5440	-18.1	Rayleigh
4	0.5630	-19.8	Rayleigh
5	0.5440	-22.9	Rayleigh
6	0.7112	-22.4	Rayleigh
7	1.9293	-15.8	Rayleigh
8	0.5133	-20.8	Rayleigh
9	1.9589	-22.6	Rayleigh
10	2.6426	-22.3	Rayleigh
11	3.7136	-25.6	Rayleigh
12	5.4524	-20.2	Rayleigh
13	12.0034	-29.8	Rayleigh
14	20.6519	-29.2	Rayleigh

* The first tap follows a Ricean distribution with a K-factor of K1 = 22 dB and a mean power of 0 dB.

TABLE 6. **Example scaling parameters for CDL and TDL models.**

Model	$DS_{desired}$ in [ns]
Very short delay spread	10
Short delay spread	30
Nominal delay spread	100
Long delay spread	300
Very long delay spread	1000

According to the actual needs of the channel simulator, it is necessary to scale the normalized delay of each tap $\tau_{n,model}$ in Table 5 to obtain the actual delay of each tap τ_n:

$$\tau_n = \tau_{n,\text{ model}} \times DS_{\text{desired}} \tag{3}$$

where $DS_{desired}$ is the Root Mean Square delay expansion factor required for scaling. In [28], example scaling parameters are given, as shown in Table 6:

Since the existence of LOS path, this paper selects the root-mean-square extension factor of short delay spread(30 ns) to implement the scaling.

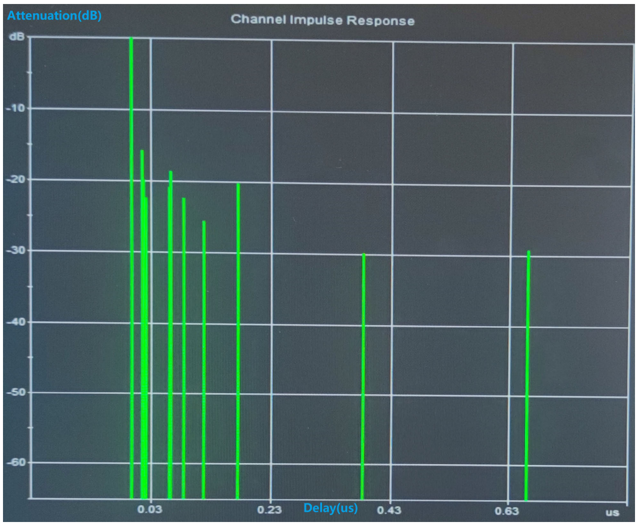

FIGURE 9. Channel Impulse Response.

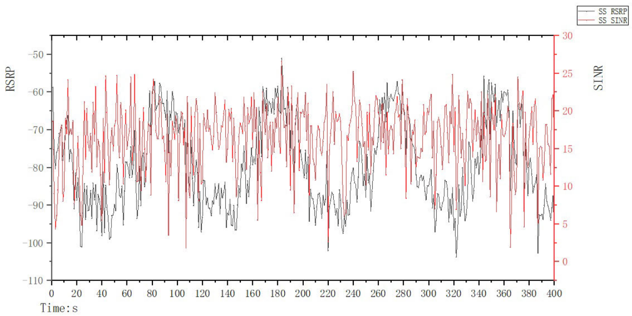

FIGURE 10. RSRP and SINR Caculated by the UE.

The small-scale model is shown in Fig. 9. The green lines represent the power and delay characteristics of different paths, the abscissa is absolute value delay, of which the unit is ns, and the ordinate is attenuation, of which the unit is dB.

The large-scale and small-scacle channel model is loaded cyclically in the time domain, and the fluctuation of the SINR and RSRP parameters obtained from the MT is shown in Fig. 10, simulating the scene of train running on the track and switching between different base stations. The power of AWGN added in the wireless channel is −120 dBm/Hz.

3) UU INTERFACE SIGNALING MONITORING TOOL

In order to analyzed the service establishment process of a MT, the Uu interface signaling monitoring tool is needed, to extract the 3GPP 5G NR RRC and NAS message with precise timestamp of the MT. Here a CDS software, which is commonly used by public network operator in their driving test, is adopted in our study. We choose a CPE that can output standard 3GPP Uu signaling which can be decoded and displayed with CDS, and the hardware of our signaling monitoring tool is shown in Fig. 11.

B. SERVICE ESTABLISHMENT LANTENCY AND TRANSITION SECTION LENGTH ANALYSIS

Service establishment process is composed with four parts, which are initialization registration, default bearing PDU establishment, dedicated PDU modification, as well as TCP/IP connection establishment. The latency of the first three parts can be derived from the CDS tool, as shown in Fig. 12:

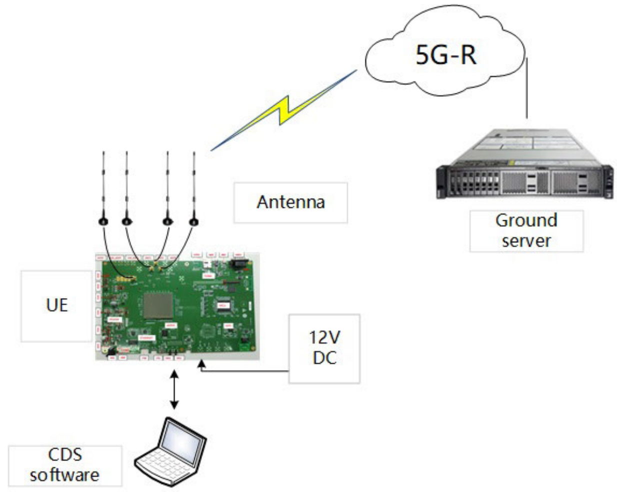

FIGURE 11. Architeture of signaling monitoring tool.

The latency of TCP/IP connection establishment can be derived from the software of Wireshark, as shown in Fig. 13:

The Service establishment latency is noded as T_{SE}, the RRC Registration Latency is noded as T_{RR}, the PDU Session Establishment Latency is noded as T_{PE}, the PDU Modification Latency is noded as T_{PM}, and the TCP/IP Connection Establishment Latency is noded as T_{TE}, the we get:

$$T_{SE} = T_{RR} + T_{PE} + T_{PM} + T_{TE} \tag{4}$$

Registration, PDU session establishment, PDU session Modification, TCP/IP connection establishment samples are obtained through testing in the typical channel environment mentioned above, and the train speed is set to 350 km/h. The 95% statistical value of latency samples of registration, PDU session establishment, PDU modification, TCP/IP connection establishment are caculated respectively. By adding the four values we get the statistical value of service establishment latency, and then the length of the transition session is caculated. The length of the transition session is noded as L_{TS}, the speed of the train is noded as V_{TS}, then we get:

$$L_{TS} = V_{TS} \times T_{SE} \tag{5}$$

C. DISTRIBUTION ANALYSIS OF PACKET LATENCY SAMPLES

TCP/IP data packets of 560 bytes are transmitted via the wireless channel with the large-scale and small-scale fading characteristics mentioned above, and the train speed is set to 350 km/h. The latency, which is approximated by half of the round trip time, is used as the sample, and 2016 samples are collected.

According to the large number theorem, when the number of samples is large, normally the sample follows normal distribution. χ^2 fitting test method is used to verify whether the

09:54:27.424	↑ N->Registration Request	NAS NR
09:54:27.424	↑ N->RRCSetupRequest	UL_CCCH_NR
09:54:27.424	↓ N->RRCSetup	DL_CCCH_NR
09:54:27.424	↓ N->CellGroupConfig	CellGroupConfig
09:54:27.440	↑ N->RRCSetupComplete	UL_DCCH_NR
09:54:27.565	↓ N->UECapabilityEnquiry	DL_DCCH_NR
09:54:27.565	↓ N->UE_CapabilityRequestFilterNR	UE-CapabilityRequestFilterNR
09:54:27.565	↑ N->UE_NR_Capability	UE-NR-Capability
09:54:27.565	↑ N->UECapabilityInformation	UL_DCCH_NR
09:54:27.628	↓ N->DLInformationTransfer	DL_DCCH_NR
09:54:27.628	↓ N->Authentication Request	NAS NR
09:54:27.628	↑ N->Authentication Response	NAS NR
09:54:27.628	↑ N->ULInformationTransfer	UL_DCCH_NR
09:54:27.722	↓ N->DLInformationTransfer	DL_DCCH_NR
09:54:27.722	↓ N->Security Mode Command	NAS NR
09:54:27.722	↑ N->Security Mode Complete	NAS NR
09:54:27.722	↑ N->ULInformationTransfer	UL_DCCH_NR
09:54:27.848	↓ N->SecurityModeCommand	DL_DCCH_NR
09:54:27.848	↑ N->SecurityModeComplete	UL_DCCH_NR
09:54:27.848	↓ N->DLInformationTransfer	DL_DCCH_NR
09:54:27.848	↓ N->Registration Accept	NAS NR

(a)

17:51:47.827	↑ N->PDU Session Establishment Request	NAS NR
17:51:47.827	↑ N->Service Request	NAS NR
17:51:47.827	↑ N->RRCSetupRequest	UL_CCCH_NR
17:51:47.859	↓ N->RRCSetup	DL_CCCH_NR
17:51:47.859	↓ N->CellGroupConfig	CellGroupConfig
17:51:47.859	↑ N->RRCSetupComplete	UL_DCCH_NR
17:51:47.920	↓ N->DLInformationTransfer	DL_DCCH_NR
17:51:47.921	↓ N->Service Accept	NAS NR
17:51:47.921	↑ N->UL NAS Transport	NAS NR
17:51:47.921	↑ N->ULInformationTransfer	UL_DCCH_NR
17:51:48.173	↓ N->SecurityModeCommand	DL_DCCH_NR
17:51:48.173	↑ N->SecurityModeComplete	UL_DCCH_NR
17:51:48.173	↓ N->UECapabilityEnquiry	DL_DCCH_NR
17:51:48.173	↓ N->UE_CapabilityRequestFilterNR	UE-CapabilityRequestFilterNR
17:51:48.173	↑ N->UE_NR_Capability	UE-NR-Capability
17:51:48.173	↑ N->UECapabilityInformation	UL_DCCH_NR
17:51:48.298	↓ N->RRCReconfiguration	DL_DCCH_NR
17:51:48.298	↓ N->CellGroupConfig	CellGroupConfig
17:51:48.314	↑ N->RRCReconfigurationComplete	UL_DCCH_NR
17:51:48.314	↓ N->DL NAS Transport	NAS NR
17:51:48.314	↓ N->PDU Session EstablishmentAccept	NAS NR

(b)

09:54:45.645	↓ N->RRCReconfiguration	DL_DCCH_NR
09:54:45.645	↓ N->CellGroupConfig	CellGroupConfig
09:54:45.645	↓ N->DL NAS Transport	NAS NR
09:54:45.645	↑ N->RRCReconfigurationComplete	UL_DCCH_NR
09:54:45.645	↓ N->PDU Session Modification Command	NAS NR
09:54:45.645	↑ N->PDU Session Modification Complete	NAS NR
09:54:45.645	↑ N->UL NAS Transport	NAS NR
09:54:45.661	↑ N->ULInformationTransfer	UL_DCCH_NR

(c)

FIGURE 12. Signaling of NAS and RRC. (a) RRC Registration Process obtained from RRC message. (b) PDU Session Establishment Process obtained from NAS message. (c) PDU Session Modification Process obtained from NAS message.

1 0.000000	172.16.11.228	10.15.94.252	TCP	66 52764 → 60001 [SYN] Seq=0 Win=64240 Len=0 MSS=1460 WS=256 SACK_PERM
2 0.047165	10.15.94.252	172.16.11.228	TCP	66 60001 → 52764 [SYN, ACK] Seq=0 Ack=1 Win=65535 Len=0 MSS=1360 WS=2048 SACK_PERM
3 0.047730	172.16.11.228	10.15.94.252	TCP	54 52764 → 60001 [ACK] Seq=1 Ack=1 Win=262400 Len=0

FIGURE 13. Process of TCP/IP establishment captured by Wireshark.

sample conforms to normal distribution, *K.Pearson* statistic is:

$$\chi^2 = \sum_{i=1}^{k} \left(\frac{v_i}{n} - p_i\right)^2 \cdot \frac{n}{p_i} = \sum_{i=1}^{k} \frac{(v_{i\text{-}n}p_i)^2}{np_i} \tag{6}$$

Considering the actual scenario, to evaluate the 5G-R network in terms of data transmission latency, the samples are obtained via the inspection train running on the track, normally the sample size may be small ($n < 30$), so the Student t-distribution is used to statistically model these latency parameter. The standard deviation σ is then replaced by the standard deviation of the sample s [32].

One of the properties of the Student t-distribution is the degree of freedom, which corresponds with the sample size. The confidence interval is denoted as:

$$\bar{x} \pm t^* \cdot \frac{s}{\sqrt{n}} \tag{7}$$

Making a choice for a deviation of 10% for $\bar{x}$, results in:

$$[0.9\bar{X}, 1.1\bar{X}] = \left[\bar{X} - t^*\frac{s}{\sqrt{n}}, \bar{X} + t^*\frac{s}{\sqrt{n}}\right] \tag{8}$$

where n is the recommended number of test samples needed to be collected during the inspection process.

D. BETTER LINK DECISION ALGORITHM DESIGN WITH INFORMER METHOD

The Informer method is adopted to build the better link decision algorithm. Informer is a transformer-based model for Long Sequence Time-Series Forecasting(LSTF) to predict long sequences [33]. The ProbSparse selfattention mechanism and distilling operation were designed to handle the challenges of quadratic time complexity and quadratic memory usage in vanilla Transformer. Also, the carefully designed generative decoder alleviates the limitation of traditional encoder-decoder architecture. The experiments on real-world data demonstrated the effectiveness of Informer for enhancing the prediction capacity in LSTF problem. The ProbSparse self-attetion formular is:

$$A(Q, K, V) = \text{Soft max}\left(\frac{\bar{Q}K^T}{\sqrt{d}}\right)V \tag{9}$$

where V is the vector representing input features, and Q and K are the eigenvectors for calculating the weight of attention. $\bar{Q}$ is the sparse matrix. And d is the input dimension. It greatly reduces the amount of calculation, and is more conducive to feature extraction and periodic information capture.

Heartbeat information is transmitted between each MT and the ground RBC, TCP/IP data packets of 560 bytes are transmitted separately via the two wireless channels. Large-scale and small-scale fading characteristics of the channels are mentioned above, and the train speed is set to 350 km/h.

The Heartbeat information latency, which is approximated by half of the round trip time, is used as the input of Informer method. And the output of Informer, which is the forecasting long sequences of the future heartbeat information latency, is further used in the better link decision algorithm.

IV. RESULTS

A. LENGTH OF TRANSITION SECTION OF HSR

Probability Density Function(PDF) of T_{RR}, T_{PE}, T_{PM} as well as T_{TE} are shown in Fig. 14:

Cumulative Distribution Function(CDF) of T_{RR}, T_{PE}, T_{PM} as well as T_{TE} are shown in Fig. 15:

The 95% statistical value of T_{RR}, T_{PE}, T_{PM} as well as T_{TE} are shown in Table 7.

The 95% statistical value of T_{SE} is noded as $T_{SE95\%}$ and calculated as:

$$T_{SE95\%} = 1534 + 1612 + 6 + 87 = 3239ms \tag{10}$$

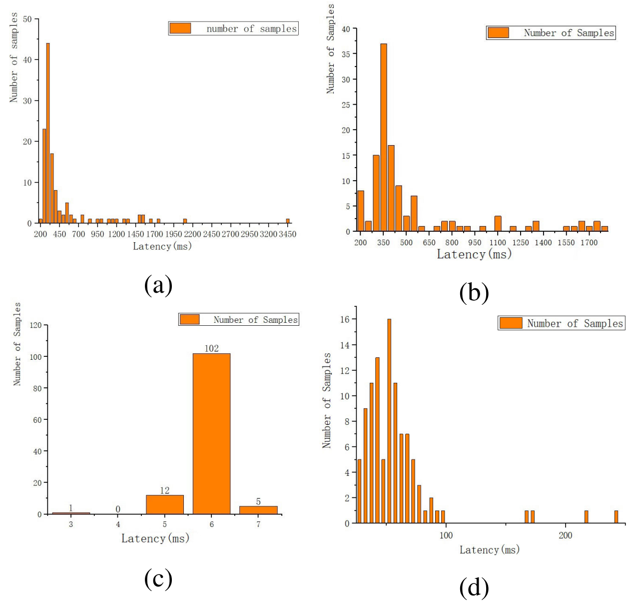

FIGURE 14. Probability Density Function(PDF) of Latency Samples. (a) RRC Registration Latency. (b) PDU Session Establishment Latency. (c) PDU Modification Latency. (d) TCP/IP Establishment Latency.

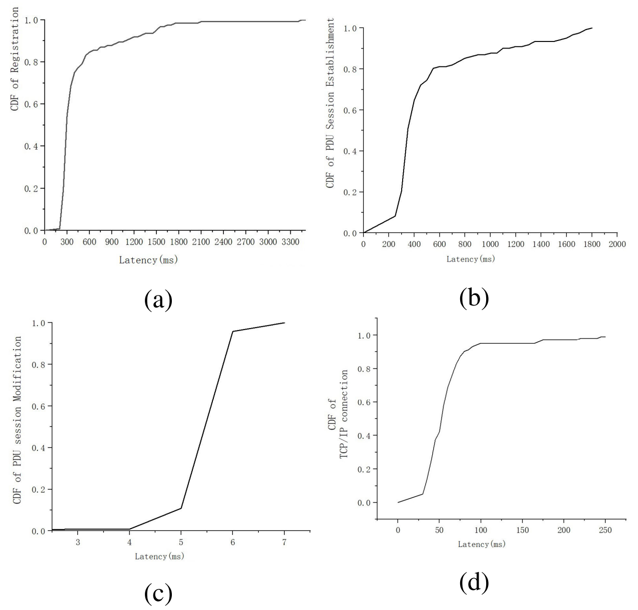

FIGURE 15. Cumulative Distribution Function (CDF) of Latency Samples. (a) RRC Registration Latency. (b) PDU Session Establishment Latency. (c) PDU Modification Latency. (d) TCP/IP Establishment Latency.

The Length of Transition Session is calculated as:

$$L_{TS} = 350km/h \times T_{SE95\%} = 350km/h \times 3239ms \approx 320m \tag{11}$$

B. PACKET LATENCY DISTRIBUTION IN TYPICAL CHANNEL SCENARIOS

The total 2016 samples are divided into 22 groups, within each group, there are at least 5 samples, to meet the requirement of χ^2 fitting test method. The Probability Density Function(PDF) of latency samples is shown in Fig. 16:

TABLE 7. 95% statistical value of T_{RR}, T_{PE}, T_{PM}, T_{TE}.

Latency	99% value in[ms]	95% value in[ms]	50% value in[ms]
Registration	2112	1534	316
PDU Establishment	1774	1612	355
PDU Modification	7	6	6
TCP/IP Establishment	245	87	53

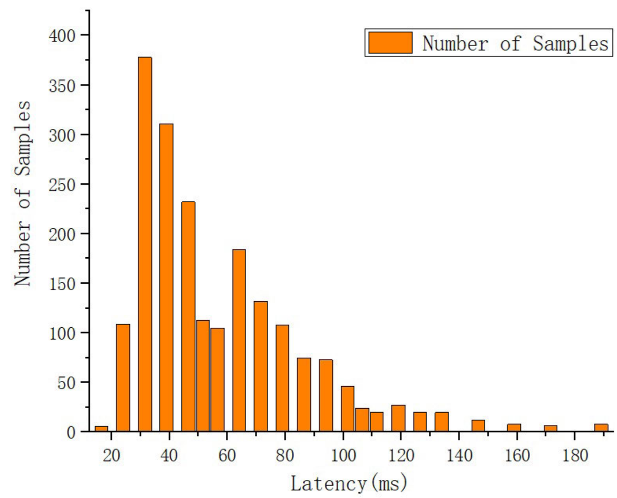

FIGURE 16. Probability Density Function (PDF) of Latency samples.

The *K.Pearson* statistic is calculated as:

$$\chi^2 = \sum_{i=1}^{k} \frac{(v_{i\text{-}n}p_i)^2}{np_i} = 5598.9845 \geq \chi^2_{1-\alpha}(k-1) \tag{12}$$

where $k = 21$, and $\alpha \in (0,1)$. So the samples do not conform to normal distribution.

Next, we use the Student t-distribution to statistically model the latency samples, and calculate the recommended test sample number in the inspection process.

$$n = \left(\frac{st^*}{0.1\bar{x}}\right)^2 \tag{13}$$

where $\bar{x} = 57.00099206$, $s = 28.82275128$, when $df = \infty$ and confidence probability is 95%, $t^* = 1.96$, using (13), we get $n \approx 98$.

Then we use $df = 98$ and confidence probability is 95%, $t^* = 1.984$, we finally get $n \approx 100$.

C. ANALYSIS OF LINK SELECTION ALGORITHM FEASIBILITY

Setting the power of AWGN added in the wireless channel to −120 dBm/Hz, which is a normal interference level, we get 2000 latency samples, the calculate window is set to 20 samples. The 2000 samples are put into the model to extract features. After the iteration is stable, 100 prediction data are

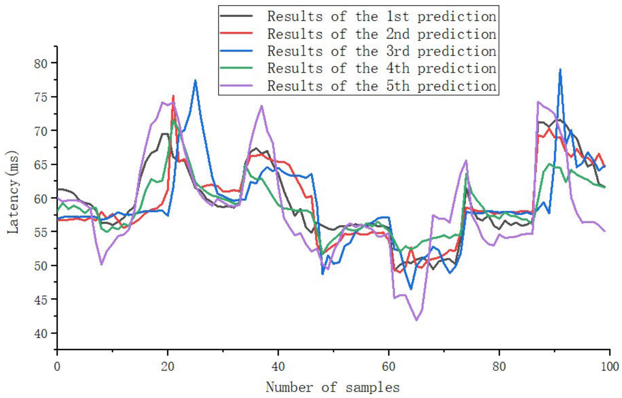

FIGURE 17. Consistency analysis of five prediction results.

TABLE 8. MSE,MAE,MAPE value of normal samples.

Prediction	MSE	MAE	MAPE
1st	4.129988	1.609	2.69%
2nd	4.494008	1.6496	2.74%
3rd	12.66821	2.5968	4.26%
4th	3.894428	1.369	2.29%
5th	16.33253	3.274	5.53%

output, and the experiment is repeated for 5 times. The results are shown in Fig. 17:

In Fig. 17, we can tell that the trends of forcasting results of 5 independent predictions are fairly similar, to further analyze the correlation degree of the five results, MSE, MAE and MAPE are calculated and shown in Table 9:

where:

$$MSE = \frac{1}{n}\sum_{i=1}^{n}\left(Y_i - \hat{Y}_i\right)^2 \quad (14)$$

$$MAE = \frac{1}{n}\sum_{i=1}^{n}\left|\left(Y_i - \hat{Y}_i\right)\right| \quad (15)$$

$$MAPE = \frac{1}{n}\sum_{i=1}^{n}\left|\frac{Y_i - \hat{Y}_i}{Y_i}\right| \times 100\% \quad (16)$$

The MAPE of each forcasting is below 20%, which indicates that the consistency of the five independent tests is good.

Now we use the former 1900 latency samples to extract features, the calculate window is still set to 20 samples. After the iteration is stable, 100 prediction data are output. Then we compare the prediction data with the latter 100 real samples. First we normalize the prediction value and the real value:

$$y = \frac{x_i - x_{\min}}{x_{\max} - x_{\min}} \quad (17)$$

As shown in Fig. 18, we can tell the prediction value and the real value have a fairly good consistency, and the effectiveness of Informer method in prediction for latency samples can be proved:

We adjust the power of AWGN to −110 dBm/Hz, and 500 abnormal latency samples are obtained. We use

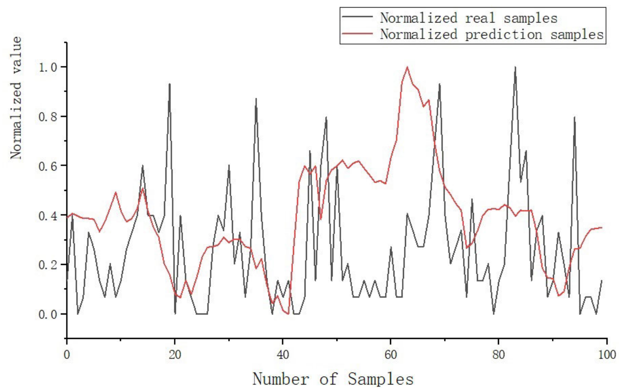

FIGURE 18. Comparison of normalized prediction and real values.

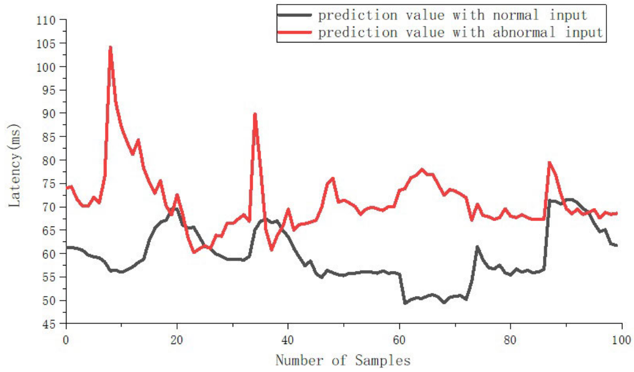

FIGURE 19. Comparison of Predictions with normal and abnormal input samples.

TABLE 9. MSE, MAE, MAPE value of abnormal samples.

MSE	MAE	MAPE
241.6449	12.8752	22.93%

1500 normal samples and 500 abnormal samples to form 2000 samples, as the input of Informer method, and predict 100 samples. Comparison of prediction results obtained with normal and abnormal input samples is shown in Fig. 19:

We can tell that when the power of AWGN is raised to −110 dBm/Hz, the prediction result of latency obviously deteriorates. MSE, MAE and MAPE are calculated again and shown in Table 9:

Here, MAPE is greater than 20%, which further proves the deterioration of the link. The result can be used to trigger the switching to the other standby wireless link, so as to maintain the continuity of train control service.

V. CONCLUSION

The service establishment time of the train control on-board modules, the end-to-end data transmission latency distribution, as well as the redundant communication link switching algorithm under network abnormal conditions, which are key points of 5G-R network bearing train control information in 350 km/h HSR, are simulated and analyzed under the built hardware-in-the-loop simulation environment combining the actual 5G-R system and channel simulator. 95%

statistical value of train control service establishment latency of 3239 ms was obtained, and a recommend transition session length of 320 m was proposed. 2016 end to end latency samples of TCP/IP protocol with 560 bytes each packet were collected. χ^2 fitting test method verifed that the samples do not conform to normal distribution, and Student t-distribution was used to statistically model the latency samples, and the recommended test sample number of 100 in the further inspection process was proposed. Based on the heartbeat information of dual MT links, Informer Long Sequence Time-Series Forecasting(LSTF) method was used to build a better link decision algorithm. The consistency and effectiveness of the algorithm were verified with normal latency samples. Then 500 abnormal samples were used as the input to the algorithm, which raised the MAPE of forecasted 100 samples up to 22.93%, and the degradation trend of the channel was successfully predicted.

Scholars are actively carrying out 5G-R channel modeling work. In the meanwhile, in China, the high-speed railway 5G-R field testing environment in under consideration and will be built in the near future. Corresponding channel model and simulation results need to be furtherly modified and verified with the presence of the HSR 5G-R environment. So the following directions of our future research are: 1) conducting wireless channel measurement and modeling in HSR 5G-R field testing environment, to obtain more tailored and accurate 5G-R large-scale and small-scale channel models. 2) furtherly verifying the relevant simulation results, as well as algorithms proposed in this paper in HSR 5G-R field testing environment.

REFERENCES

[1] *UIC ERTMS*. Accessed: Jan. 15, 2023. [Online]. Available: https://uic.org/rail-system/ertms/

[2] *UIC FRMCS*. Accessed: Jan. 15, 2023. [Online]. Available: https://uic.org/rail-system/frmcs/

[3] *5G Industry and Market Development Report*, TDIA, Beijing, China, 2022.

[4] FRMCS Functional Working Group. (2020). *Future Railway Mobile Communication System User Requirements Specification (V5.0.0)*. Accessed: Jan. 28, 2023. Paris, France. [Online]. Available: https://uic.org/rail-system/frmcs/

[5] S. F. Ruesche, J. Steuer, and K. Jobmann, "The European switch," *IEEE Veh. Technol. Mag.*, vol. 3, no. 3, pp. 37–46, Sep. 2008, doi: 10.1109/MVT.2008.927490.

[6] Y. Yu, "Research on key technologies of train-ground communication for CTCS-3 train control service based on 5G-R," M.S. thesis, Dept. Elect. Eng., Beijing Jiaotong Univ., Beijing, China, 2021.

[7] J. Ding, J. Song, S. Lin, Y. Cao, and Z. Zhong, "Feasibility of train-ground safety data transmission for CTCS-3 train control system based on GPRS packet switching network," *China Railway Sci.*, vol. 36, no. 3, pp. 119–126, May 2015.

[8] *Description and Evaluation of Possible FRMCS Migration Variants for Existing ETCS and Cab Radio On-Board Units*. Accessed: Jan. 28, 2023. [Online]. Available: https://uic.org/IMG/pdf/description_and_evaluation_of_possible_of_possible_frmcs_migration_variants_for_existing_etcs_and_cab_radio_on-board_units-toba_7515-v1.2.pdf

[9] *Railway Gazette*. Accessed: Mar. 6, 2023. [Online]. Available: https://www.railwaygazette.com//krri-tests-5g-based-autonomous-train-control/57534.article

[10] R. He, B. Ai, Z. Zhong, A. F. Molisch, R. Chen, and Y. Yang, "A measurement-based stochastic model for high-speed railway channels," *IEEE Trans. Intell. Transp. Syst.*, vol. 16, no. 3, pp. 1120–1135, Jun. 2015, doi: 10.1109/TITS.2014.2328493.

[11] T. Zhou, H. Zhang, B. Ai, C. Xue, and L. Liu, "Deep-learning-based spatial–temporal channel prediction for smart high-speed railway communication networks," *IEEE Trans. Wireless Commun.*, vol. 21, no. 7, pp. 5333–5345, Jul. 2022, doi: 10.1109/TWC.2021.3139384.

[12] B. Ai, X. Cheng, T. Kürner, Z. Zhong, K. Guan, R. He, L. Xiong, D. W. Matolak, D. G. Michelson, and C. Briso-Rodriguez, "Challenges toward wireless communications for high-speed railway," *IEEE Trans. Intell. Transp. Syst.*, vol. 15, no. 5, pp. 2143–2158, Oct. 2014, doi: 10.1109/TITS.2014.2310771.

[13] J. Ding, W. Jiang, Z. Zhong, K. Guan, and B. Ai, "Measurement and analysis of Doppler shift for high-speed rail scenario," *High Technol. Lett.*, vol. 21, no. 2, pp. 192–199, Jun. 2015, doi: 10.3772/j.issn.1006-6748.2015.02.011.

[14] Z. Mo, M. Wang, and Z. Zhao, "Radio communication protocol design and difference analysis of CTCS-3 train control system based on GSM-R and 5G-R," *Railway Standard Des.*, vol. 67, no. 11, pp. 1–6, Nov. 2023, doi: 10.13238/j.issn.1004-2954.202205050003.

[15] Y. Zhou, "Applicability study on CTCS-3 train control system based on 5G-R," *China Railway*, pp. 94–99, Sep. 2022, doi: 10.19549/j.issn.1001-683x.2022.04.10.002.

[16] H. Xie, "Research on new generation of train control communication system based on 5G technology," *Technol. Innov.*, vol. 18, no. 12, pp. 38–45, Dec. 2021, doi: 10.3969/j.issn.1673-4440.2021.12.008.

[17] L. Zhu, D. Yao, and H. Zhao, "Reliability analysis of next-generation CBTC data communication systems," *IEEE Trans. Veh. Technol.*, vol. 68, no. 3, pp. 2024–2034, Mar. 2019, doi: 10.1109/TVT.2018.2870053.

[18] K. T. P. Nguyen, J. Beugin, M. Berbineau, and M. Kassab, "A new analytical approach to evaluate the critical-event probability due to wireless communication errors in train control systems," *IEEE Trans. Intell. Transp. Syst.*, vol. 18, no. 6, pp. 1380–1392, Jun. 2017, doi: 10.1109/TITS.2016.2604043.

[19] L. Li, K. Xu, D. Wang, C. Peng, K. Zheng, R. Mijumbi, and Q. Xiao, "A longitudinal measurement study of TCP performance and behavior in 3G/4G networks over high speed rails," *IEEE/ACM Trans. Netw.*, vol. 25, no. 4, pp. 2195–2208, Aug. 2017, doi: 10.1109/TNET.2017.2689824.

[20] J. Wang, Y. Zheng, Y. Ni, C. Xu, F. Qian, W. Li, W. Jiang, Y. Cheng, Z. Cheng, Y. Li, X. Xie, Y. Sun, and Z. Wang, "An active-passive measurement study of TCP performance over LTE on high-speed rails," in *Proc. 25th Annu. Int. Conf. Mobile Comput. Netw.*, Los Cabos, Mexico, Aug. 2019, pp. 1–13.

[21] L. Lei, L. Jiahua, J. Yuming, S. Xuemin, L. Ying, Z. Zhangdui, and L. Chuang, "Stochastic delay analysis for train control services in next-generation high-speed railway communications system," *IEEE Trans. Intell. Transp. Syst.*, vol. 17, no. 1, pp. 48–64, Jan. 2016, doi: 10.1109/TITS.2015.2450751.

[22] X. Zhang, H. Li, and Q. Guo, "Research on smooth transition scheme of 5G-R and GSM-R network train dispatching communication services," *Railway Standard Des.*, vol. 66, no. 10, pp. 166–171, Oct. 2022, doi: 10.13238/j.issn.1004-2954.202107130007.

[23] *Technical Specification Group Radio Access Network; NR; Radio Resource Control (RRC) Protocol Specification*, 3GPP, document TS 38.331, 2022.

[24] *Technical Specification Group Core Network and Terminals; Non-Access-Stratum (NAS) Protocol for 5G System (5GS)*, 3GPP, document TS 24.501, 2022.

[25] *Subset-037 3.2.0, Euroradio FIS*, UNISIG, Brussels, Belgium, 2015.

[26] *Subset-093 3.0.14, GSM-R Interfaces Bearer Service Requirements*, UNISIG, Brussels, Belgium, 2016.

[27] *Subset-026 2.3.0, System Requirements Specification*, UNISIG, Brussels, Belgium, 2006.

[28] *Technical Specification Group Radio Access Network; Study on Channel Model for Frequencies From 0.5 to 100 GHz*, 3GPP, document TS 38.901, 2022.

[29] T. Zhou, H. Zhang, B. Ai, and L. Liu, "Weighted score fusion based LSTM model for high-speed railway propagation scenario identification," *IEEE Trans. Intell. Transp. Syst.*, vol. 23, no. 12, pp. 23668–23679, Dec. 2022, doi: 10.1109/TITS.2022.3191338.

[30] Li Anning, Li Hui, and L. Yiqun, "Large scale channel modeling for railway dedicated 5G network railway," *Standard Des.*, vol. 66, no. 8, pp. 162–167, Aug. 2022, doi: 10.13238/j.issn.1004-2954.202105200001.

[31] *Guidelines for Evaluation of Radio Interface Technologies for IMT-2020*, document M.2412-0, ITU-R, Oct. 2017.

[32] *ERTMS/GSM-R Quality of Service Test Specification*, document O-2475 3.0, UIC ERTMS, 2007.

[33] H. Zhou, S. Zhang, J. Peng, S. Zhang, J. Li, H. Xiong, and W. Zhang, "Informer: Beyond efficient transformer for long sequence time-series forecasting," 2020, *arXiv:2012.07436*.

YIQUN LIANG received the B.E. and M.E. degrees from Beijing Jiaotong University (BJTU), Beijing, China, in 2005 and 2007, respectively. He is currently pursuing the Ph.D. degree in information engineering and control with the China Academy of Railway Sciences. He is also a Researcher with the Signal and Communication Research Institute, China Academy of Railway Sciences. He has done some research in the field of railway radio propagation and application and testing system of both GSM-R and the next generation radio-communication systems, for past 17 years. He mainly engages in the research of railway communication and long-term follows up ITU and UIC meetings.

HUI LI received the B.E. degree from the Department of Electronic Engineering, Beihang University, in 1991. Since July 1991, he has been with the Institute of Communication and Signal, China Academy of Railway Sciences. In March 2010, his technical title was promoted to a researcher. He guides students' scientific research as a doctoral supervisor. He has engaged in the research, standard formulation, product development, scientific experiment, new technology promotion, and the application of railway communication technology, for more than 30 years. In recent years, he has mainly engaged in the research of new generation mobile communication technology for railway.

YI LI received the Ph.D. degree from Southwest Jiaotong University, in 2018. He is currently an Associate Researcher with the Signal and Communication Research Institute, China Academy of Railway Sciences, Beijing, China. His research interests include wireless channel measurement and modeling, interference management, and electromagnetic compatibility.

ANNING LI received the B.E. degree from Southwest Jiaotong University, Chengdu, China, in 2019, and the M.E. degree from the China Academy of Railway Sciences, Beijing, China, in 2022. She is currently a Research Intern with the Institute of Signal and Communication, China Academy of Railway Sciences, mainly engaged in railway communication research.

YUNQI WANG received the B.E. degree from Beijing Jiaotong University (BJTU), Beijing, China, in 2021. He is currently a Graduate Student with the China Academy of Railway Sciences. He mainly engages in the research of railway communication.

DE LI received the M.E. degree from the University of Electronic Science and Technology of China, in 2003. He is currently with the Signal and Communication Research Institute, China Academy of Railway Sciences, mainly engaged in the research of railway communication. He has long-term followed up the CCSA meeting, with more than 20 years of experience in telecommunication speciation developing and product developing and testing.